

Cancer Detection using Deep Learning

Anand Kumar
M.Tech CSE - MT23111
IIITD
anand23111@iiitd.ac.in

I. PROBLEM STATEMENT

The detection of metastatic tissue in histopathologic images is a critical task in medical diagnosis, particularly for cancer detection. The PatchCamelyon (PCam) dataset is a valuable resource for training machine learning models to perform this task. This report details the approach and results of developing a Convolutional Neural Network (CNN) to classify images from the PCam dataset, indicating the presence of metastatic tissue.

II. MOTIVATION

The field of digital pathology is developing rapidly, following recent advancements in microscopic imaging hardware that allow digitizing glass slides into whole-slide images (WSIs). This digitization has facilitated image analysis algorithms to assist and automate diagnostic tasks. A proven approach is to use convolutional neural networks (CNNs), a type of deep learning model, trained on patches extracted from whole-slide images. The aggregate of these patchbased predictions serves as a slide-level representation used by models to identify metastases, stage cancer or diagnose complications. This approach has been shown to outperform pathologists in a variety of tasks

III. LITERATURE REVIEW

The application of deep learning techniques, particularly Convolutional Neural Networks (CNNs), to medical image analysis has seen significant advancements over the past decade. This literature review will provide an overview of key studies and developments in the field, focusing on the detection of metastatic tissue in histopathologic images.

A. Deep Learning for Medical Image Analysis

1) *Early Developments:* Early machine learning applications in medical imaging concentrated on feature extraction methods and traditional algorithms like random forests and support vector machines (SVMs). Nevertheless, these techniques were constrained by their dependence on manually generated features and the challenge of identifying the intricate patterns found in medical pictures.

2) *Emergence of Deep Learning:* The emergence of deep learning for image classification has revolutionized the field of computer vision, transforming how machines interpret visual data. This progress is attributed to several key developments and breakthroughs in machine learning and neural network research. The field of image analysis was completely transformed by CNNs. Given that CNNs can automatically learn hierarchical features from raw pixel data, tasks like object detection, segmentation, and picture classification are especially well suited for CNNs.

B. CNN Model Architecture

A Convolutional Neural Network (CNN) is a type of artificial neural network commonly applied to analyzing visual imagery. It's particularly effective for tasks like image recognition and classification.

1) *Convolutional Layers:* These layers apply convolution operations to the input image, using learnable filters (also known as kernels) to extract features like edges, textures, and patterns. The filters slide over the input image, producing feature maps that highlight relevant spatial information.

2) *Activation Function:* Typically, each convolutional layer is followed by an activation function like ReLU (Rectified Linear Unit), which introduces non-linearity to the network, enabling it to learn complex patterns and relationships in the data.

3) *Pooling Layers:* Pooling layers downsample the feature maps, reducing their spatial dimensions while retaining important information. Common pooling operations include max pooling and average pooling, which help to make the representation more compact and computationally efficient.

4) *Fully Connected Layers:* After several convolutional and pooling layers, the network may have one or more fully connected layers. These layers connect every neuron from the previous layer to every neuron in the subsequent layer, allowing the network to learn high-level features and make predictions based on the extracted features.

5) *Softmax Layer:* In classification tasks, the softmax layer is often used as the output layer. It applies the softmax function

to the output of the last fully connected layer, converting the raw scores into probabilities. Each output neuron represents the probability of a particular class, and the predicted class is the one with the highest probability.

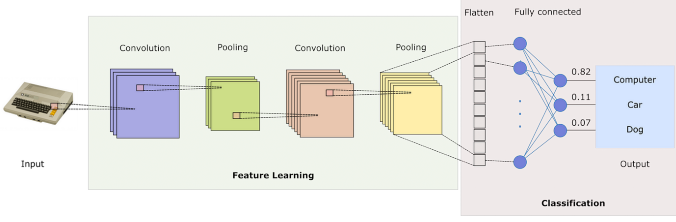


Fig. 1. CNN ARCHITECTURE

6) *Training*: CNNs are trained using labeled data through a process called backpropagation, where the network adjusts its parameters (such as weights and biases) to minimize the difference between predicted and actual outputs. This is typically done using optimization algorithms like stochastic gradient descent (SGD) or its variants.

IV. DATASET DETAILS

A. PatchCamelyon(PCam)

The PatchCamelyon benchmark is a new and challenging image classification dataset. It consists of 327,680 color images (96 x 96px) extracted from histopathologic scans of lymph node sections. Each image is annotated with a binary label indicating presence of metastatic tissue.

B. Numbers

The dataset is divided into a training set of 2,62,144 (2^{18}) examples, and a validation and test set both of 32,768 (2^{15}) examples. There is no overlap in WSIs between the splits, and all splits have a 50/50 balance between positive and negative examples.

C. Labeling

A positive label indicates that the center 32x32px region of a patch contains at least one pixel of tumor tissue. Tumor tissue in the outer region of the patch does not influence the label. This outer region is provided to enable the design of fully-convolutional models that do not use any zero-padding, to ensure consistent behavior when applied to a whole-slide image.

D. Patch selection

PCam is derived from the Camelyon16 Challenge [2], which contains 400 H&E stained WSIs of sentinel lymph node sections. The slides were acquired and digitized at 2 different centers using a 40x objective (resultant pixel resolution of 0.243 microns). We undersample this at 10x to increase the field of view. We follow the train/test split from the Camelyon16 challenge [2], and further hold-out 20% of the train WSIs for the validation set. To prevent selecting background

patches, slides are converted to HSV, blurred, and patches filtered out if maximum pixel saturation lies below 0.07 (which was validated to not throw out tumor data in the training set). The patch-based dataset is sampled by iteratively choosing a WSI and selecting a positive or negative patch with probability p . Patches are rejected following a stochastic hard-negative mining scheme with a small CNN, and p is adjusted to retain a balance close to 50/50.

E. Data Format

The images and labels are stored in gzipped HDF5 files. The patches were selected using a stochastic hard-negative mining scheme to balance the dataset.

V. VISUALIZATIONS

A. Confusion Matrix

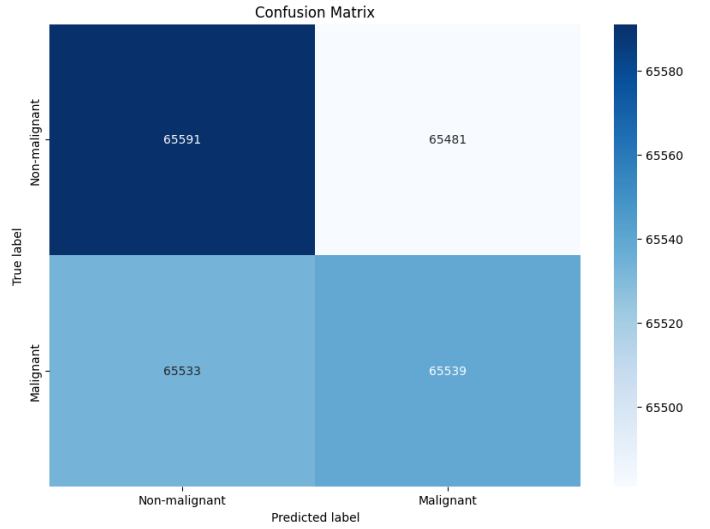


Fig. 2. Confusion-Matrix

B. ROC Curve

C. precision-recall curve

D. $CNN_{accuracy}$

VI. RESULTS

The results of the model evaluation on the test set are as follows:

A. *Test Loss*: [0.8489215689187404]

B. *Test Accuracy*: [81.2652587890625]

These results demonstrate the model's effectiveness in detecting metastatic tissue in histopathologic images. The use of data augmentation and dropout layers helped in achieving better generalization and reducing overfitting.

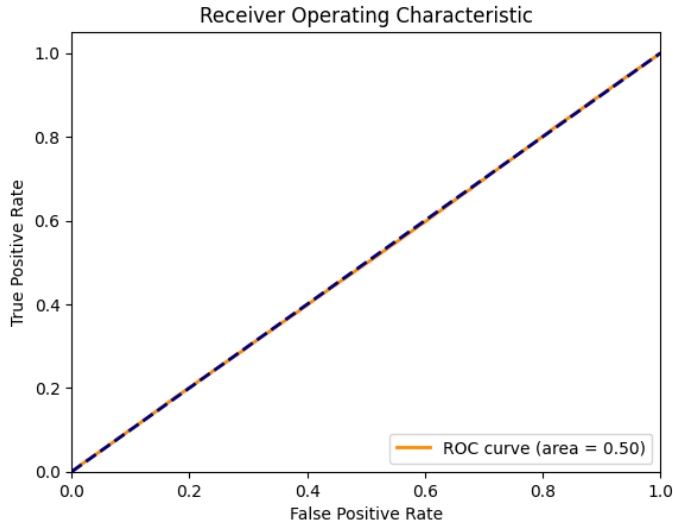


Fig. 3. ROC curve

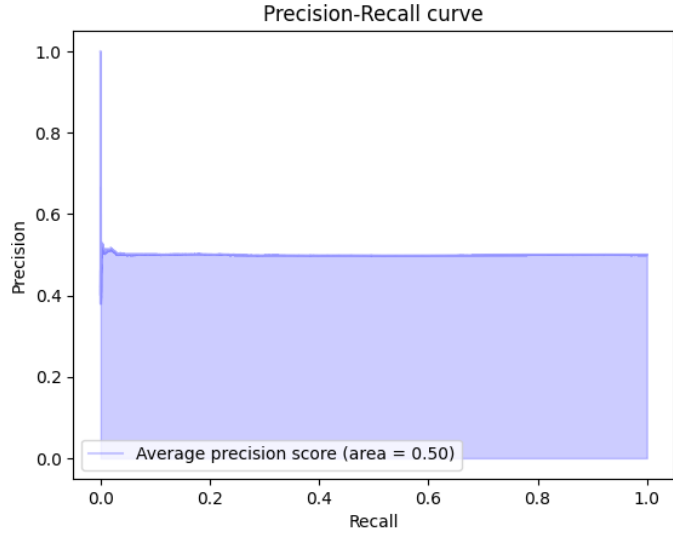


Fig. 4. precision-recall curve

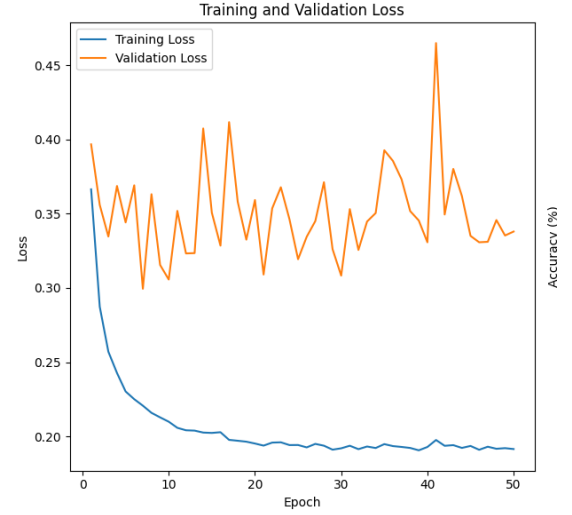


Fig. 6. Validation Loss

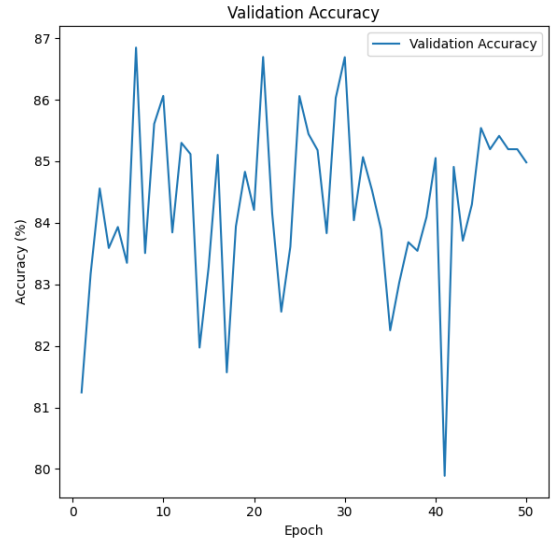


Fig. 7. Validation Accuracy

Epoch [17/50],	Loss: 0.19767635181142396,	Val Loss: 0.4116881161899073,	Val Accuracy: 81.5704345783125%
Epoch [18/50],	Loss: 0.19789183244531434,	Val Loss: 0.3581024923187215,	Val Accuracy: 83.941658398625%
Epoch [19/50],	Loss: 0.19645800814495762,	Val Loss: 0.33252899784086904,	Val Accuracy: 84.8297119140625%
Epoch [20/50],	Loss: 0.19522804995360476,	Val Loss: 0.3592228561549766,	Val Accuracy: 84.218205878125%
Epoch [21/50],	Loss: 0.193812594017254495,	Val Loss: 0.3894857132381069,	Val Accuracy: 86.6943359375%
Epoch [22/50],	Loss: 0.19694799187074633,	Val Loss: 0.35360702548052214,	Val Accuracy: 84.1552234375%
Epoch [23/50],	Loss: 0.19604804665337888,	Val Loss: 0.3678389827837236,	Val Accuracy: 82.55615234375%
Epoch [24/50],	Loss: 0.1941791815888436,	Val Loss: 0.34634073183406144,	Val Accuracy: 83.612808546875%
Epoch [25/50],	Loss: 0.1942280280468633,	Val Loss: 0.3193539621133823,	Val Accuracy: 86.8595703125%
Epoch [26/50],	Loss: 0.1926181146172884,	Val Loss: 0.3344626719481312,	Val Accuracy: 85.43115234375%
Epoch [27/50],	Loss: 0.194971488753372737,	Val Loss: 0.3458699280133209,	Val Accuracy: 85.188648625%
Epoch [28/50],	Loss: 0.1937521938894838,	Val Loss: 0.37123216621694155,	Val Accuracy: 83.831787189375%
Epoch [29/50],	Loss: 0.19188949418261603,	Val Loss: 0.3261418164122354,	Val Accuracy: 86.029652734375%
Epoch [30/50],	Loss: 0.19199453768938923,	Val Loss: 0.38838543819692414,	Val Accuracy: 86.6912841796875%
Epoch [31/50],	Loss: 0.19372501118587292,	Val Loss: 0.35386868602047436,	Val Accuracy: 84.0423833984375%
Epoch [32/50],	Loss: 0.191424882838282925,	Val Loss: 0.32598518314138684,	Val Accuracy: 85.8677488234375%
Epoch [33/50],	Loss: 0.19321852168379538,	Val Loss: 0.34472449294116814,	Val Accuracy: 84.527587890625%
Epoch [34/50],	Loss: 0.19219644545848873,	Val Loss: 0.3584492738135898,	Val Accuracy: 83.889785678125%
Epoch [35/50],	Loss: 0.19482183267882647,	Val Loss: 0.39275164177524857,	Val Accuracy: 82.254028326125%
Epoch [36/50],	Loss: 0.192489122147112,	Val Loss: 0.3858187073542835,	Val Accuracy: 83.032265625%
Epoch [37/50],	Loss: 0.1922216818853364,	Val Loss: 0.3732111529388837,	Val Accuracy: 83.686382734375%
Epoch [38/50],	Loss: 0.19224187329382403,	Val Loss: 0.3517695891722999,	Val Accuracy: 83.544921875%
Epoch [39/50],	Loss: 0.19864652290126105,	Val Loss: 0.3454338728563946,	Val Accuracy: 84.09423826125%
Epoch [40/50],	Loss: 0.19289472117361584,	Val Loss: 0.3307482154858376,	Val Accuracy: 85.85480234375%
Epoch [41/50],	Loss: 0.197595165459461,	Val Loss: 0.4049380258124156,	Val Accuracy: 79.888916815625%
Epoch [42/50],	Loss: 0.19368338146897899,	Val Loss: 0.3494847977780205,	Val Accuracy: 84.989856171875%
Epoch [43/50],	Loss: 0.19412596349502564,	Val Loss: 0.3881784451279673,	Val Accuracy: 83.789716796875%
Epoch [44/50],	Loss: 0.1922672974836774,	Val Loss: 0.36189596449548844,	Val Accuracy: 84.2987868546875%
Epoch [45/50],	Loss: 0.19388576456761512,	Val Loss: 0.3358635347385797,	Val Accuracy: 85.548771484375%
Epoch [46/50],	Loss: 0.19180754177977819,	Val Loss: 0.3397726779021233,	Val Accuracy: 85.1959228515625%
Epoch [47/50],	Loss: 0.19387474242417155,	Val Loss: 0.331898947651954,	Val Accuracy: 85.41228765625%
Epoch [48/50],	Loss: 0.1916864178418833,	Val Loss: 0.3457384974581348,	Val Accuracy: 85.1959228515625%
Epoch [49/50],	Loss: 0.1912812890379643,	Val Loss: 0.3352655774615705,	Val Accuracy: 85.1959228515625%
Epoch [50/50],	Loss: 0.1914957545361586,	Val Loss: 0.337999648400003,	Val Accuracy: 84.982298046875%
Test Loss: 0.848921569117484			
Test Accuracy: 81.2652457080625%			

Fig. 5. ROC curve

C. Validation Loss

D. Validation Accuracy

E. Autoencoders Loss-Validation Loss curve

VII. CONCLUSION

From this project we learnt that .Research in this area has been accelerated by CNNs' performance in contests like Camelyon16 and the creation of datasets like PCam, which show how these methods have the ability to complement and even exceed human diagnostic abilities. It is probable that forthcoming studies will persist in enhancing existing models, investigating innovative frameworks, and using more extensive and varied datasets in order to augment the precision and dependability of computerized cancer detection systems.

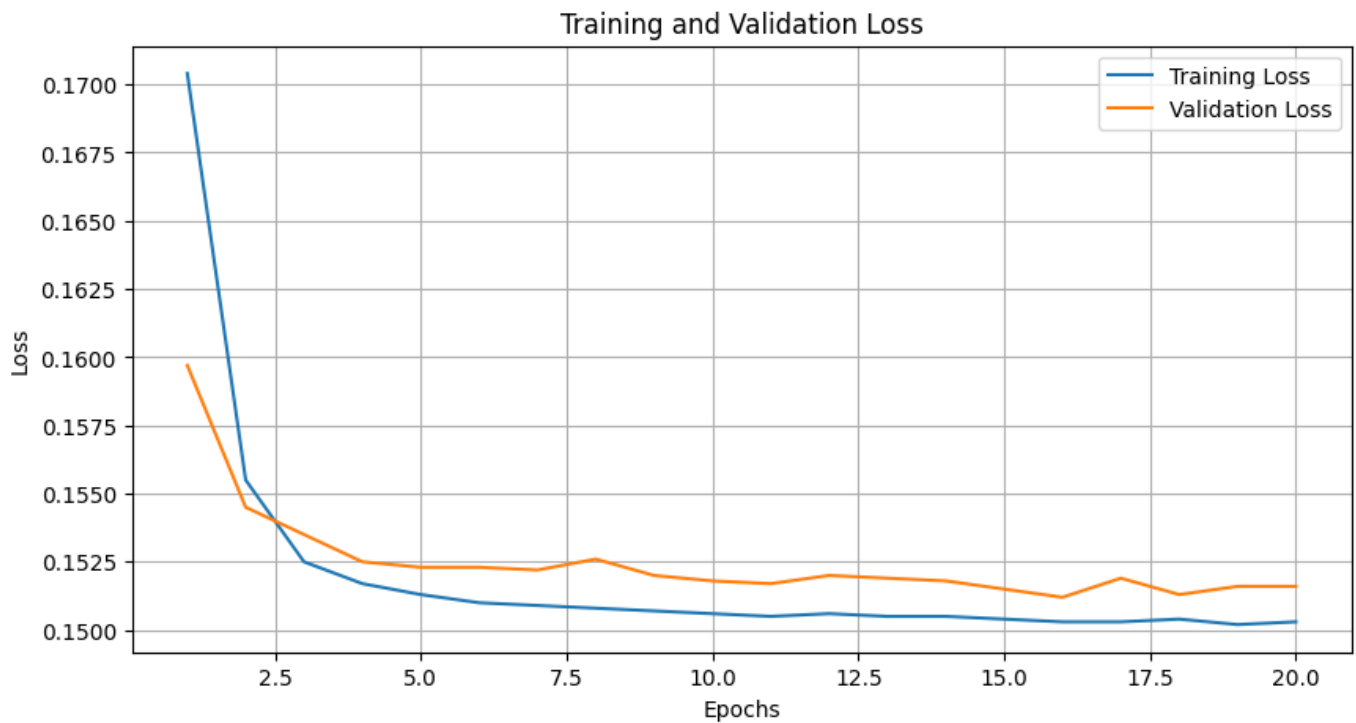


Fig. 8. Autoencoders Loss-Validation Loss curve

REFERENCES

- [1] B. S. Veeling, J. Linmans, J. Winkens, T. Cohen, M. Welling. "Rotation Equivariant CNNs for Digital Pathology". arXiv:1806.03962
- [2]. Matek, C., Schwarz, S., Marr, C., Spiekermann, K. (2019). A Single-cell Morphological Dataset of Leukocytes from AML Patients and Non-malignant Controls [Data set]. The Cancer Imaging Archive. <https://doi.org/10.7937/tcia.2019.36f5o9ld>
- [3]. Alagu, S., Bagan, K. B. (2019). Acute lymphoblastic leukemia diagnosis in microscopic blood smear images using Texture features and SVM classifier.